*atmosphere*

MDPI

*Review*

# State of the Art of Martian Weather–Climate Modeling and Open Challenges

**Edoardo Bucchignani**

Centro Italiano Ricerche Aerospaziali (CIRA), Via Maiorise, 81043 Capua, Italy; e.bucchignani@cira.it

**Abstract**

Mars climatology is a growing interest domain for planetary research and for operational missions. In the last three decades, Martian General Circulation Models have been developed to support the interpretation of spacecraft and telescopic observations and for the advancement of theoretical understanding of the climate. They have been designed to represent key processes, such as dust cycle, seasonal $CO_2$ condensation, and interaction between boundary layer and surface. At the same time, new observations from orbiters and landers have enhanced the diagnostics, but several uncertainties in the parameterization, especially in dust representation and turbulent mixing, require further improvements. This review represents a synthesis of the state of the art of existing global and regional models, comparing numerical and physical approaches, identifying the main challenges for the next years, with particular attention to the needs of operational missions and machine learning techniques.

**Keywords:** Martian atmosphere; climate modeling; GCM; state of the art

## 1. Introduction

In the XXI century, Mars explorations moved from pure geological recognition to the systematic characterization of climate and atmosphere. Mariner 4 (1964) and Viking 1,2 (1975) missions marked the first successes in the exploration of Mars, providing the first images and analyses of the soil. After the space missions of the 1970s, the general circulation of Mars has become the best known after the terrestrial one. In fact, on both planets, a large amount of solar radiation reaches the surface, and the thermal radiation heats the atmosphere [1]. In 1996, the NASA Mars Pathfinder was the first mission to carry a rover (Sojourner) to the planet. The lander operated as a weather station, while the rover analyzed the soil and rocks at the landing site and performed various experiments on the surface. The Mars Science Laboratory (MSL) is a NASA exploration mission, mainly made up of Curiosity Rover activities, launched on 26 November 2011, landed on 6 August 2012, and is currently ongoing.

Operational requirements related to rovers, landers, and future assets require reliable weather forecasting and a deep understanding of climate processes that regulate the seasonal and interannual variability of the planet. General Circulation Models (GCMs) developed for Mars (LMD, NASA/Ames, MarsWRF) are useful tools to support missions and research activities. However, they often do not converge on specific topics, due to uncertainties on dust-lifting parameterizations, dust optical properties, and planetary boundary layer representation. This review aims to provide an updated overview of modeling architecture, available observations, and critical areas that need rapid developments, with the aim of providing the community with shared research planning.

Check for updates

Academic Editor: Elizabeth A. Silber

Received: 14 April 2026
Revised: 14 May 2026
Accepted: 15 May 2026
Published: 18 May 2026

**Copyright:** © 2026 by the author. Licensee MDPI, Basel, Switzerland. This article is an open access article distributed under the terms and conditions of the Creative Commons Attribution (CC BY) license.

The modeling of the Martian atmosphere started in 1969 with Leovy and Mintz [2], who adapted the Mintz–Arakawa two-level model for planetary atmospheres under Martian conditions. The most important variations were the removal of oceans and mountains and the change in composition of the atmosphere. They performed two experiments, simulating respectively orbital conditions at the southern summer solstice and at the southern autumnal equinox. Successively, this model was updated at the NASA AMES Research Center [3], incorporating the radiative effects of atmospheric dust on solar and thermal radiation, and used for the simulation of the general circulation of the Martian atmosphere. Several numerical experiments were conducted for alternative choices of seasonal date and dust optical depth.

In 1989, the LMD terrestrial climate model was adapted to Mars with the introduction of a new radiative transfer module and a parameterization of $CO_2$ condensation and sublimation [4]. This model was validated against pressure measurements provided by Viking and temperature fields provided by Mariner-9. In the 1990s, a spectral solver in conjunction with a simplified set of parameterizations was implemented at the Universities of Reading and Oxford [5], while an advanced version of the LMD model was developed thanks to a joint effort of the Laboratoire de Meteorologie Dynamique (LMD, France) and the Department of Atmospheric, Oceanic and Planetary Physics of Oxford University (AOPP, United Kingdom) [6].

On Mars, deterministic forecasts can be made for only 3–5 Martian days (Sol), due to the limited availability of observations from rovers and sensors, consequently limiting assimilation. By comparison, even terrestrial numerical weather prediction systems, which assimilate a larger amount of data, are generally subject to a deterministic predictability limit of about 7–10 days due to the chaotic nature of atmospheric dynamics. Nowadays, Martian weather forecasts are useful to plan rover activities (Perseverance, Curiosity, Opportunity, Spirit), avoid dust storms that could damage solar panels, estimate visibility and energy production, and forecast wind and turbulence for drones (e.g., Ingenuity). Before landing, local weather is simulated around the landing area by evaluating density, wind, temperature, and turbulence. The main centers providing weather forecasts are NASA (USA), supporting Perseverance and Curiosity, LMD (France), providing forecasts for lander, orbiter, and future missions, and ESA (Europe), providing information to support European missions.

An exhaustive review about existing Martian climate models was presented in 2003 by Lewis [7], providing a comprehensive assessment of the theoretical framework, numerical methods, and physical parameterizations available at the time. In the last two decades, the field has undergone substantial transformation, since advances in computational power have enabled higher spatial resolution, multiscale nesting approaches, and more complex representations of radiative transfer and aerosol–dynamics coupling. At the same time, a large amount of observational data from missions such as Mars Global Surveyor (MGS), Mars Reconnaissance Orbiter (MRO), Mars Express, MAVEN, and multiple landed platforms have profoundly reshaped our understanding of Martian atmospheric structure and variability. The present work aims to provide an updated perspective, building upon the foundations laid two decades ago and reflecting the substantial progress achieved since.

The literature review was conducted using Scopus, Web of Science and Google Scholar. The search focused on studies related to Martian GCMs and their applications to the simulation of the Martian climate. The main search terms included Mars GCM, Martian General Circulation Model, Mars climate modeling, Mars atmospheric dynamics, Mars dust cycle, Mars mesoscale modeling and Mars atmospheric simulations. Additional searches were performed for specific topics such as dust storms, radiative transfer, atmospheric data assimilation, and Entry, Descent, and Landing (EDL) applications.

The review mainly considered peer-reviewed articles published between 2000 and 2025, with particular attention to studies describing the development, validation, and scientific applications of Martian GCMs. Conference proceedings and technical reports were included when directly relevant to operational or mission-related applications.

This paper is organized as follows: Section 2 describes the main Martian atmospheric features. Section 3 provides an overview of existing operating GCMs, and Section 4 briefly discusses limited-area models and high-resolution studies. Finally, Section 5 provides a discussion about open challenges, while the main conclusions are presented in Section 6.

## 2. Martian Atmospheric Features

Mars is significantly smaller than Earth, its diameter being about half of the terrestrial one (6787 km vs. 12,742 km) and its mass about 1/10 that of the Earth. Martian atmosphere is composed almost entirely of carbon dioxide, specifically $CO_2$ 95%, $N_2$ 2.7%, and Argon 1.6% with traces of oxygen and water vapor [8]. Weather features have been analyzed through data provided by space probes, orbiters, and rovers and through results of numerical simulations. Mars climate is variable in time and space, due to diurnal and seasonal cycles, combined with variable topography. Despite its low density, Mars is characterized by strong winds (in the order of tens of km/h) and ice clouds, along with $CO_2$ snow. The surface pressure is very low (about 7 mb), meaning less gas than on Earth is available to absorb radiation and heat transfer. Since the mass content is low, due to the scarce thermal inertia, the soil warms up mainly during the daytime and quickly cools down at nighttime. Moreover, for the same reason, dust represents the main element for radiative balance control. In fact, during global dust storms, almost all the solar radiation is absorbed in the atmosphere and the soil remains cool. $CO_2$ creates a greenhouse effect only at nighttime due to its capacity to absorb infrared radiation from soil, while the radiative effects of ozone layer are generally negligible [9]. The average surface temperature is about −60 °C. Due to the low thermal capacity of the atmosphere, diurnal and seasonal variations in temperature are higher with respect to Earth, being about 60 °C on Mars and 30 °C on Earth, with peaks of 90 °C in the Martian polar regions, whilst seasonal variations in daily mean surface air temperature reach up to about 50 °C in the extreme terrestrial climate of northeastern Siberia [1]. In a clear atmosphere, heating from the surface generates convection extending up to approximately one pressure scale height (H). The pressure scale height depends on atmospheric temperature and gravity and represents the vertical distance over which pressure decreases by a factor $e$. Using typical near-surface temperatures, H is about 7.5 km for Earth and about 10 km for Mars. In this convective boundary layer, temperature decreases by about 4.3 °C per km. At higher altitudes, temperature decreases more gradually, reaching the $CO_2$ condensation values (−143 °C to −123 °C) at about 40 km. General circulation is driven by horizontal temperature values associated with pressure variations.

GCMs are mainly used for generating climatology over many years. A year on Mars is equivalent to 687 Earth days [10]. A Martian day (sol) is only slightly longer than an Earth day: 24 h and 39 min. Instead of months, solar longitude (from 0 to 360°) is used, which is the position of Mars along its orbit around the Sun. The Martian calendar began much more recently than that on Earth: years are counted from the spring equinox in the planet's northern hemisphere, which occurred on 11 April 1955, marking the beginning of Martian year 1. In 2026, the current year on Mars is 38.

## 3. An Overview of Existing Operating GCMs

In the last three decades, several GCMs have been developed for the simulation of the Martian atmosphere, generally obtained starting from numerical cores designed for the representation of Earth climate. Climate models incorporate orographic information

obtained from mission datasets. A map of Mars and its related orography, with major regions labeled, is shown in Figure 1.

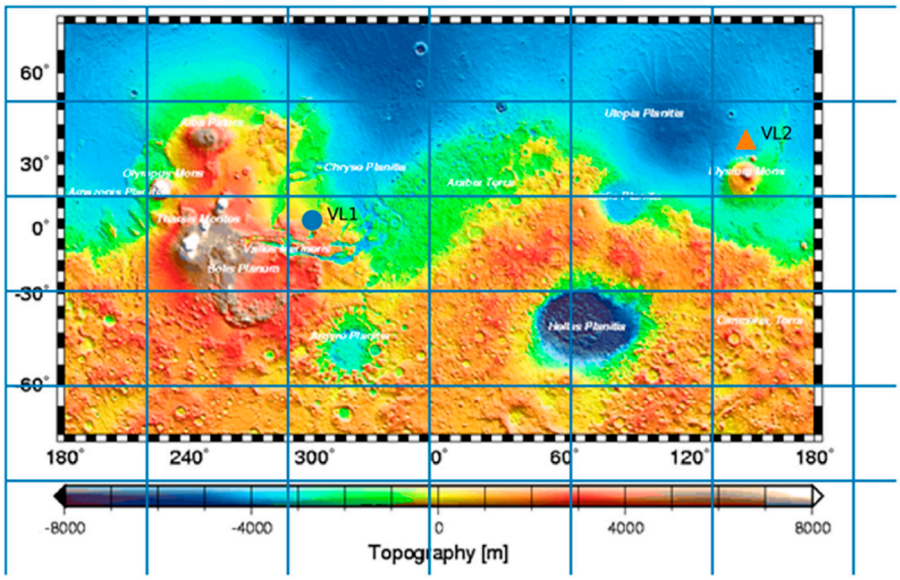



**Figure 1.** Global topographic map of Mars based on Mars Orbiter Laser Altimeter (MOLA) data. The locations of Viking Lander 1 (VL1) and Viking Lander 2 (VL2) are indicated. Image credit: NASA Goddard Space Flight Center (GSFC), available at https://attic.gsfc.nasa.gov/mola/images/topo_labeled.jpg, accessed on 17 March 2026).

### *3.1. General Information About Martian GCMs*

The governing equations of a Martian GCM are the same as for a terrestrial model, but the physical terms in the equations are different, due to the distinct features of the Martian atmosphere. Specifically, the values of the specific gas constant $R_s$, of the gravity acceleration, of density and of specific heats are different. Moreover, an additional term is present in the continuity equation, since $CO_2$ condensates directly, and a specific transport equation is included for the dust. The main differences between Earth and Mars GCMs lie in the physical parameterizations, since physical processes are different:

- Turbulence, due to the different planetary boundary layer (PBL) heights (1–2 km on Earth, 10 km on Mars for the strong diurnal thermal gradients that enhance convection).
- Convection, which is moist on Earth and dry on Mars.
- Radiative transfer, due to a different atmospheric composition.
- Clouds, related to water and ice on Earth, and to $CO_2$ ice on Mars.
- Different surface heat exchange: oceans and vegetation on Earth, dry soil on Mars.

### *3.2. LMD Mars GCM*

The LMD Mars GCM [6] was developed at Laboratoire de Meteorologie Dinamique (LMD, France) with the support of the Department of Atmospheric, Oceanic and Planetary Physics (AOPP) of Oxford University and is widely used, especially for the development of the Mars Climate Database (MCD). It is employed for climate simulations covering many Martian years, for the execution of sensitivity studies, and for the development of climatological datasets (i.e., MCD). The model has been recently renamed as "Mars Planetary Climate Model" [11] and is freely distributed and available to the community through the website http://www-planets.lmd.jussieu.fr/ (accessed on 9 March 2026).

The model includes a hydrodynamical part for the resolution of the general equations of atmospheric circulation and a physical part specific to this planet. The hydrodynamical code is based on the spatial and temporal integration of the equations of fluid dynamics on

a three-dimensional grid, starting from an initial state. It adopts a finite difference discretization of the governing equations on a longitude–latitude grid and a vertical discretization based on a terrain-following coordinate system. The horizontal resolution typically ranges from 5° to 1°, but it is possible to increase the number of grid points to zoom in on a given part of the globe, such as at the spacecraft landing sites. The top layer is positioned at a height of about 100 km. Typical computational grids are characterized by $64 \times 48 \times 25$ or $64 \times 48 \times 32$ or $32 \times 42 \times 25$ grid points. Given that the Martian radius is about 3400 km, the grid $64 \times 48$ corresponds to cells of 330 km $\times$ 220 km at the equator. Vertical levels are distributed in a non-uniform way to obtain the largest accuracy near the soil. The calculations are performed by means of horizontal exchanges among cells. The physical part can be seen as a juxtaposition of several columns of atmosphere.

The radiative transfer parameterization computes atmospheric heating and cooling rates as well as the surface radiative fluxes by accounting for the absorption and scattering of solar (shortwave) and thermal (longwave) radiation. The radiative processes are treated using a correlated-k method, which provides an efficient representation of spectrally resolved gas absorption in a $CO_2$-dominated atmosphere. Thermal infrared emission and near-infrared solar absorption by $CO_2$ are explicitly considered. For thermal infrared, the strong 15 μm $CO_2$ band is treated using a wide-band approach, which captures the main features of absorption and emission. The model includes Doppler broadening effects that become important at high altitudes (above ~50 km), while non-local thermodynamic equilibrium effects are not considered. The absorption of solar radiation in the near-infrared $CO_2$ bands is represented through a simplified parameterization. Although this process is negligible in the lower atmosphere, it becomes more important above 50 km and contributes significantly to atmospheric heating.

Atmospheric dust plays a key radiative role by absorbing and scattering parts of solar radiation, heating the layers where it has a larger concentration, and reducing the flux that reaches the soil. Moreover, dust emits infrared radiation, influencing nighttime temperature. These processes are modeled with the numerical scheme of Fouquart and Bonel [12], originally developed for terrestrial GCM, while the scattering of thermal infrared radiation initially was not considered, according to most Earth studies. However, in [6], it was found that for many wavelengths the infrared radiation scattered by the atmospheric dust back to the surface cannot be neglected, as it causes a change in surface and atmospheric temperature. For this reason, a scheme that accounts for multiple scattering by dust particles outside the 15 μm $CO_2$ band was included. The evolution of surface temperature is described as a balance between incoming fluxes and soil thermal conduction, using an 11-layer soil model.

The PBL is represented with a turbulence closure based on prognostic turbulent kinetic energy to allow the simulation of extremely deep PBLs (8–10 km) and shallow nocturnal stable layers, typical of Mars. Finally, a standard energy conserving convective adjustment scheme is used, which mixes heat and momentum in convectively unstable layers.

In the LMD Mars GCM, data assimilation relies on a nudging scheme to incorporate observations, e.g., temperature profiles from Mars Climate Sounder (MCS), dust optical depth from Thermal Emission Spectrometer (TES), and surface pressure from landers, constraining the simulated Martian atmosphere.

The model has been employed for the realization of the MCD [13], developed to provide a realistic modelization of the Martian climate system. The MCD provides average values and statistics of the main meteorological variables (temperature, density, pressure, wind) and atmospheric composition (dust, water vapor, ice content) at resolution $5.675° \times 3.75°$. It can be used in the context of specific studies requiring an accurate description of the state of the Martian atmosphere. Since the main factor influencing

Martian climate is dust load, the MCD provides a series of climatologies for different dust scenarios: standard year, cold (low dust), hot (high dust), and dust storm. Moreover, the database provides additional "add-on" scenarios focusing on individual Martian years (24 to 31), which are useful to reproduce specific historical conditions or for comparison with missions/experiments performed in a selected year. The fields are saved 12 times a day, approximately every 2 Martian hours, to describe the diurnal cycle appropriately. The latest version of the database (6.1) is freely distributed through the website https://www-mars.lmd.jussieu.fr/ (accessed on 9 March 2026). The MCD has been validated against observational data from many available sources (e.g., Viking landers). An example of temperature distribution over the Martian surface, extracted from the MCD [14], is shown in Figure 2.

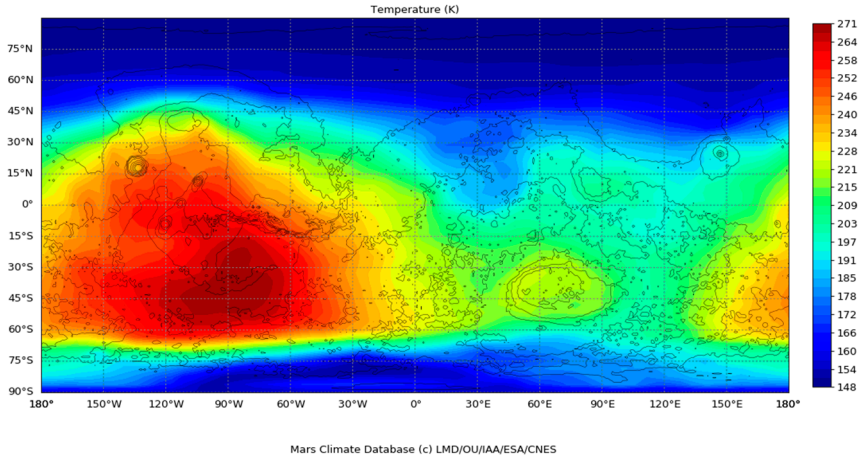



**Figure 2.** Temperature distribution of the Martian surface for Mars year 38, Ls = 245.5°, sol 477. Extracted from the Mars Climate Database (Laboratoire de Météorologie Dynamique, LMD, https://www-mars.lmd.jussieu.fr/, accessed on 16 March 2026) [14].

The model was also used to explore the possible climate of Mars in the past, when obliquity was different [11], and also used for providing environmental predictions aimed at preparing space missions, e.g.,

- Mars Express: Space exploration by ESA of the planet and its moons since 2003. It includes the Mars Express Orbiter and Beagle 2, a lander designed to perform exobiology and geochemistry research (https://www.esa.int/Science_Exploration/Space_Science/Mars_Express, accessed on 9 March 2026).
- ExoMars Rover (now named Rosalind Franklin) designed for the ExoMars mission by ESA; expected to launch in 2028 (https://www.esa.int/Science_Exploration/Human_and_Robotic_Exploration/Exploration/ExoMars/ExoMars_rover, accessed on 9 March 2026).

### *3.3. NASA AMES Mars M-GCM*

The M-GCM was developed by the Mars Climate Modeling Center (MCMC) at the National Aeronautics and Space Administration (NASA, USA) to support operational missions in the 2000s and is continuously updated. It is also used for multimodel intercomparison, studies on interannual variability, and density forecasting. The model has played a central role in the interpretation of spacecraft observations and in the advancements of the theoretical understanding of Martian climate dynamics since the Viking era. Its development started with early global circulation experiments described by Haberle [15], which established the basics of modern Mars climate modeling.

The M-GCM solves the hydrostatic dynamical equations on a rotating sphere using finite-difference techniques and a terrain-following coordinate in the vertical direction. The horizontal resolutions ranges from $5^\circ \times 6^\circ$ to $1^\circ \times 1^\circ$, with 30–50 vertical levels extending up to 80–100 km altitude, depending on the application.

The physical parameterization packages include a $CO_2$ radiative transfer, surface–atmosphere exchange, and aerosol processes, allowing the reproduction of the strong seasonal and diurnal variability characteristic of Mars. Radiative forcing is treated using schemes that account for infrared cooling by $CO_2$ and heating by airborne dust. Dust lifting, transport and sedimentation are represented in an interactive way or by using prescribed scenarios. In this way, the M-GCM can simulate both climatological dust cycles and episodic global dust storms. Surface processes are simulated through parameterizations of thermal inertia, albedo, and topographic forcing, including high-resolution datasets derived from spacecraft measurements. The representation of polar $CO_2$ condensation and sublimation allows a realistic simulation of seasonal mass exchange between atmosphere and surface, which is a feature of Martian climate.

The M-GCM is characterized by a data assimilation system able to incorporate data from the Mars Color Imager (MARCI), TES, MCS, land pressure, and temperature measurements, allowing the short-range forecasts (2–5 sol) to support rover operations as well as Entry, Descent, Landing studies.

The model is currently used for practical applications, thanks to the effort provided at MCMC [16], aimed at updating NASA missions and operating support. Specifically, the model provides forecasts for Entry, Descent, and Landing (EDL) of landers such as:

- Phoenix (2008): wind and density at 68° N during Martian summer.
- InSight (2018): density profiles and shear winds at Elysium Planitia.
- Mars 2020/Perseverance (2021): evaluation of Terrain-Relative Navigation and parachute deployment, integrated with data MCS for dust storms [17].
- Future ones (e.g., Mars Sample Return).

It is also employed in near-real-time aerobraking operations for missions such as MGS, Odyssey, and MRO to provide forecasts of atmospheric density along the braking corridors.

Data are distributed through the NASA Ames web interface (https://data.nas.nasa.gov/mcmc/portals/web-interface/, accessed 10 March 2026). Moreover, the MCMC made available the Community Analysis Pipeline (CAP) [18], an open-source Python-based command line tool for analyzing and visualizing M-GCM output. An example of temperature distribution over the Martian surface generated with this model is shown in Figure 3.

The model has also been employed for scientific research. Batterson et al. [19] reproduced the recurring southern polar "B" regional dust storm observed by TES on MGS and by MCS on MRO. Their simulations showed that during years without global dust storms, the B storm over the retreating south polar $CO_2$ cap is driven by repeated dust plumes poleward of 70° S. Hinson and Wilson [20] analyzed seven years of temperature profiles from the MCS to characterize atmospheric waves generated by boundary-layer winds over steep topography. A complementary simulation with the M-GCM was then used to interpret the observations and better understand the generation and structure of waves in the Martian atmosphere. The Mars year 34 global dust storm (June 2018) was monitored by several spacecraft in orbit and was modeled with M-GCM in [17], to understand its evolution and assess sources and sinks of dust.

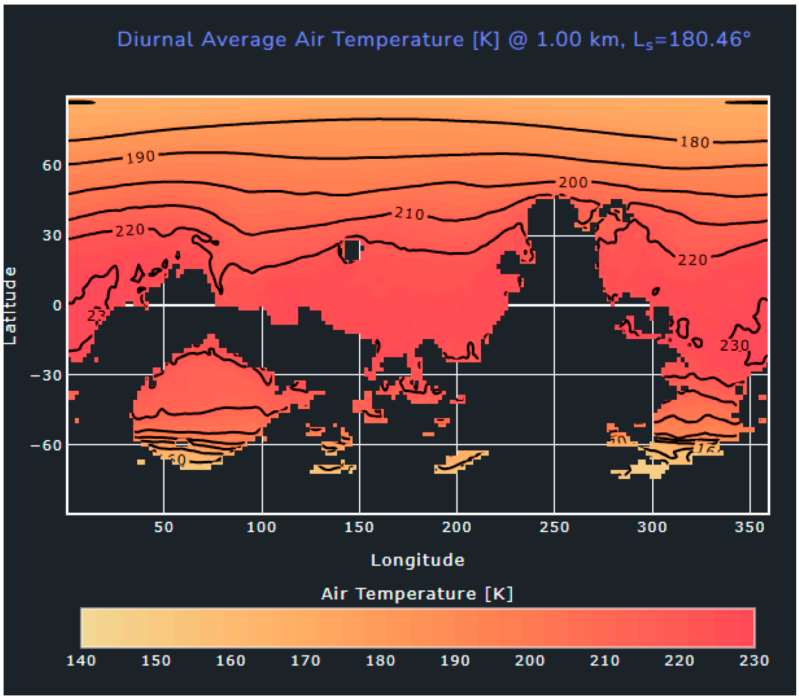



**Figure 3.** Diurnally averaged air temperature at 1 km altitude (Ls ≈ 180°). Plot generated using the NASA NAS Data Portal (MCMC interface). NASA data are in the public domain. (https://data.nas.nasa.gov/mcmc/portals/web-interface/ accessed on 19 March 2026).

### *3.4. MarsWRF*

The MarsWRF (Mars Weather Research and Forecasting model) [21] is a Mars-specific implementation of the planetWRF model [22], which was adopted from the terrestrial WRF model. It is used to simulate the mesoscale circulation, regional dust storms, characterization of landing sites, and study of boundary layer processes. Maintained through a collaboration between NASA Ames, the Spanish Research Council (CSIC), and others, it enables mesoscale-to-microscale modeling of Martian weather, bridging the gap between GCMs like NASA Ames M-GCM and local observations from landers and rovers.

MarsWRF is characterized by a fully compressible, non-hydrostatic dynamical core, supporting nested grids and regional domains with spatial resolution of less than 10 km, allowing the study of regional phenomena not completely solved by GCMs (see Section 4). The parameterization schemes of the terrestrial model have been modified to adapt to Martian conditions, particularly dry convection, PBL schemes, and interactive dust transport (via moment method), while the fast accurate radiative transfer model was developed in 2012 [23]. The $CO_2$ scheme allows a portion of the atmosphere to freeze out onto the surface if any point in the vertical column becomes super-saturated and allows $CO_2$ to sublime back into the atmosphere if the atmosphere over $CO_2$ ice becomes sub-saturated [24]. The model supports fully coupled dust cycles, predicting lifting, transport, and sedimentation with sub-grid variability. Additional key physics include water ice microphysics, regolith heat diffusion, and boundary-layer schemes tuned for Mars' thin atmosphere (about 1% Earth density). An interesting feature is that MarsWRF can be coupled to Large Eddy Simulation (LES) configurations for explicit simulation of turbulence and convective structures, as described in [25].

The model assimilates data for initialization from missions like MGS using the Data Assimilation Research Testbed (DART) [26], a rigorous framework that allows various observation types to be combined using a common interface to an Ensemble Kalman

Filter. Data from other missions, e.g., MRO, Phoenix, Curiosity and InSight, can also be assimilated.

In [21], the sensitivity of the model to the horizontal resolution was investigated considering grids from 7.5° × 9° to 0.5° × 0.5°, encompassing a wide range from standard Mars GCMs to global mesoscale modeling. It was found that while most of the gross-scale circulation features are insensitive to horizontal resolution, several major features are sensitive, e.g., the northern winter polar circulation. A high number of Rover Environmental Monitoring Station (REMS) wind measurements were collected in three science investigations during MSL's Bagnold Dunes Campaign and compared with numerical modeling with MarsWRF [24], considering over 80 sols around southern winter solstice (Ls ∼90°). Zhou et al. [27] also investigated the impact of model horizontal resolution of the model by increasing the commonly used value 5° × 5° to the higher value 3° × 3°, applying an interactive dust scheme to parameterize the dust-lifting process. They found that increasing the horizontal resolution with interactive dust produces only limited changes in the simulated climate. Relevant differences emerged only in regions characterized by complex topography, such as Olympus Mons, the Hellas Basin, and the southern cap-edge areas. Figure 4 shows the vertical cross-section of five-sol-averaged zonal-mean temperature (K) around Ls = 0° in the standard resolution (5° × 5°) and high-resolution (3° × 3°) simulations. The analysis of results suggests that higher horizontal resolution is particularly important for the investigation of regions with complex terrain. Conversely, in flat areas, e.g., the Tianwen-1 landing site in Utopia Planitia, simulations performed at standard resolution tend to provide comparable results while requiring substantially lower computational resources.

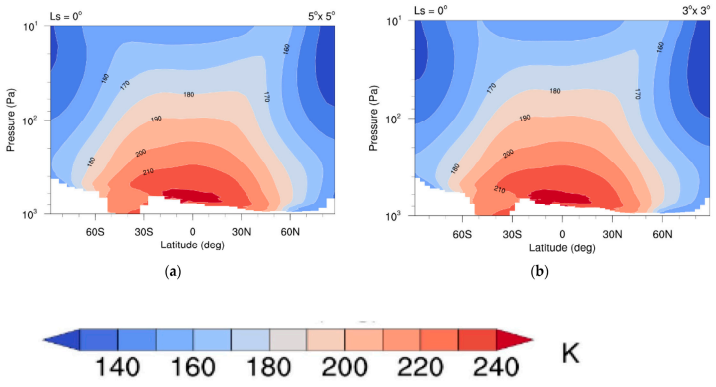



**Figure 4.** Vertical cross-section of five-sol-averaged zonal-mean temperature (K) around Ls = 0° in (**a**) the standard-resolution (5° × 5°) and (**b**) high-resolution (3° × 3°) simulations. Reproduced from Zhou et al. (2022) [27], under the terms of the Creative Commons Attribution (CC BY 4.0) license.

In [28], the model was run in a five-nest configuration, down to a spatial resolution of about 1.46 km, centered on the landing sites of six past missions. It was found that the model reproduces accurately the EDL vertical profiles in terms of density, temperature, pressure, and horizontal wind in the lowest 30 km, where the most critical phase of the EDL takes place.

### *3.5. UK Met Office Mars Unified Model*

The UK Met Office has recently adopted the Unified Model (UM) to deal with Martian applications [29]. This effort is notable because the UM underpins both operational weather forecasting and climate simulations on Earth, offering a unified approach across scales. Even if it is less mature than LMD or MarsWRF, the UM-Mars model highlights the feasibility of transferring state-of-the-art Earth system modeling infrastructure to planetary atmospheres. A highly sophisticated model was created by adapting established climate

schemes used for the study of Earth to the specific features of Mars (e.g., atmospheric dust, wind, atmospheric composition) [30].

The Global Atmosphere 7.0 science configuration of the UM was adapted to Martian conditions. The computational core is based on a non-hydrostatic fully compressible flow solver, which uses a semi-implicit timestep and semi-Lagrangian advection scheme. The model incorporates a dynamic dust scheme that explicitly reproduces saltation processes, allowing for a more realistic simulation of dust lifting and transport. Surface properties are treated through a roughness length derived from [31], ensuring consistency with observed Martian terrain features. The Martian orography is described, including a smoothing of extreme elevations, with maximum and minimum surface heights ranging between +8.2 and −8.2 km, respectively, to maintain numerical stability. An average surface pressure of about 610 Pa is assumed, representing typical Martian conditions, and adopting a simplified atmospheric composition of 95% $CO_2$ and 5% $N_2$, neglecting the contribution of argon. An idealized $CO_2$ ice scheme is included to account for seasonal condensation and sublimation processes, which dynamically modify surface pressure through mass exchange between the atmosphere and polar caps. Additionally, the model represents Martian moisture quantities, enabling the simulation of water-related processes. The data assimilation scheme is based on techniques designed to interface with models of different complexity, capable of analyzing any randomly distributed dataset [32].

In [29], a resolution of 2° in latitude and 2.5° in longitude (grid size of 118 km × 147.5 km at the equator) was used, along with 50 hybrid-height atmospheric levels up to a model top of 80 km above the areoid level. Model output was validated against in situ data from the Viking landers and output from the LMD Mars GCM. As an example, Figure 5 shows the surface pressure at Viking Lander 1 and Viking Lander 2 sites over a Martian year, provided by observational data [33] and model output. It is shown that the cold season pressure drop present in observations is not represented by the model, since UM does not currently have a $CO_2$ ice cycle.

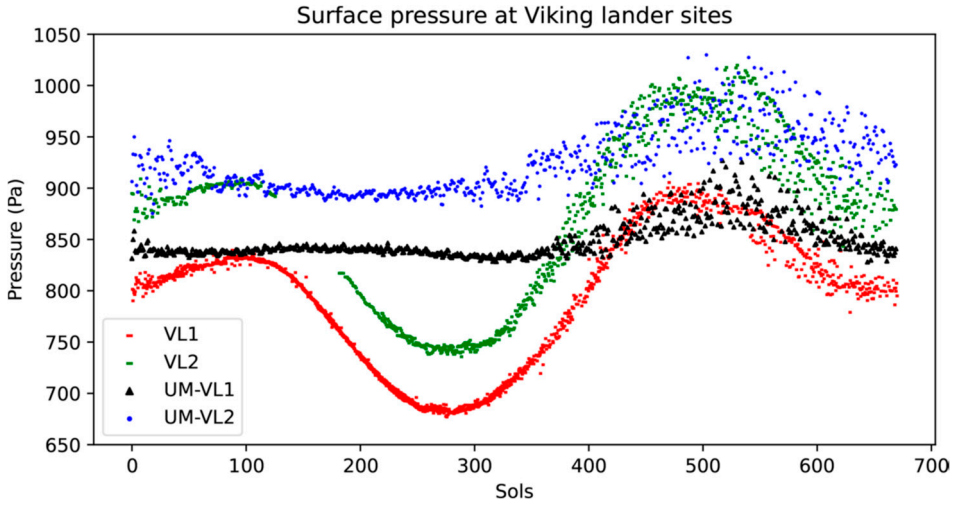



**Figure 5.** Surface pressure at approximate Viking Lander 1 and Viking Lander 2 sites over a Martian year. Reproduced from McCulloch et al. (2023) [29] under the Creative Commons Attribution 4.0 License. Viking lander observational data from Tillman (1989) [33].

Overall, UK Met Office model demonstrated good capabilities in reproducing the main features of large-scale Martian circulation but lacks two important physical processes, i.e., water and $CO_2$ cycle.

As a summary of this section, which provided an overview of the main GCMs, Table 1 presents a comparison of the main features of the different models.

**Table 1.** Main features of different Mars climate models.

| | **LMD GCM** | **NASA M-GCM** | **MarsWRF** | **Met Office UM** |
|---|---|---|---|---|
| Institute | LMD (France) | MCMC (USA) | NASA AMES (USA), CSIC (Spain) | UK Met Office |
| Main Focus | Mars Climate Database | Support for operations missions | Mesoscale/Microscale modeling | Research |
| Dynamical core | Hydrostatic | Hydrostatic | Non-Hydrostatic | Non-Hydrostatic |
| Discretization | Finite difference on a 3D grid | Finite difference on a rotating sphere | Finite difference on Arakawa C-grid | Finite difference on Arakawa C-grid |
| Data assimilation | Nudging scheme. Data from MCS, TES, landers | Ensemble Kalman filter. Data from MARCI, TES, MCS | Data Assimilation Research Testbed | Three-Dimensional Variational Assimilation |

## 4. Limited-Area Models and High-Resolution Studies

GCMs have some limitations in simulating local climate, since they are characterized by resolutions around or coarser than 100 km, while important phenomena occur at spatial scales less than 10 km. Moreover, GCMs do not adequately account for complex topography, which is an important aspect of the physical response governing the regional/local atmospheric features. Thus, downscaling techniques and Regional Climate Models (RCMs) were developed in the early 1990s for terrestrial applications [34] and have since developed rapidly and significantly. They take the large-scale predictions provided by GCMs and extract the implied information at more regional/local scales. In recent years, limited-area models (meso- and microscale) have been applied not only to Earth applications, but also to the Martian atmosphere to support the interpretation of in situ measurements from landed spacecraft and to investigate meteorological processes occurring at sub-global scales. The spatial resolutions employed, down to hundreds of meters, allow LES approaches where boundary-layer dynamics can be explicitly resolved [35]. The lateral boundary conditions for such limited-area models must either be provided by output from GCM archives or, in the case of idealized experiments, specified as periodic.

Early regional simulations were performed employing the Mars Regional Atmospheric Modeling System (MRAMS) model [36], which descended from the Regional Atmospheric Modeling System (RAMS), to be largely used among the terrestrial community in the late 1990s. RAMS is a non-hydrostatic and not fully compressible model, based on grid-volume Reynolds-averaged primitive equations. The pressure signal modeled using the baseline RAMS dynamical core, in the absence of full compressional heating, is unable to properly reproduce the strong diurnal pressure cycles of Mars. For this reason, a correction was performed by adding the compressional term (i.e., a term proportional to the time rate of change in potential temperature) to the dynamical core, substantially improving the simulation of Mars' diurnal pressure cycles. An additional buoyancy term was also added. The height coordinate system is based on a terrain influenced geometric approach. In regards to physical parameterizations, the model uses foreground dust and background dust fields individually (or in combination) to simulate a wide variety of scenarios. The cloud microphysics scheme employed is the Community Aerosol and Radiation Model for Atmospheres (CARMA) model adapted for Mars $H_2O$ ice and $CO_2$ ice clouds. In [36], MRAMS simulations covering the Mars Pathfinder landing site were performed, using a grid with 55 $\times$ 55 points horizontally (grid spacing of 60 km) and 47 points in the vertical direction. Initial and boundary conditions (updated every six hours) were obtained from the NASA Ames M-GCM. The simulation started before sunrise (0530 local time) at $L_s = 142^\circ$, covering approximately 3 sols. Model evaluation, conducted against Pathfinder data, revealed good capabilities of the model, even if maximum temperatures were slightly underpredicted, as well as wind speeds. Interestingly, the model revealed that the Martian

atmosphere is about two–three times more turbulent than the terrestrial atmosphere in the afternoon, but with fluxes that are an order of magnitude smaller, due to the lower density. Successively, the model was updated and the current version (v2.9_r39) was presented in detail in [37]. Apart from technical updates to modern Fortran standards, the full compressibility was included in the model core, along with a complete linearization of the buoyancy term, to guarantee a proper representation of the strong irrotational flows associated with the atmospheric tide. Overall, this version can represent the main key physical processes and can be applied to any geographical area, from pole to equator, differently from the original model that was only capable of simulating the very basic mesoscale and microscale circulations. Figure 6 shows the Olympus Mons cloud particle distribution at several locations to the lee of the volcano, simulated with MRAMS as an example of the modeled microphysical details of the afternoon clouds.

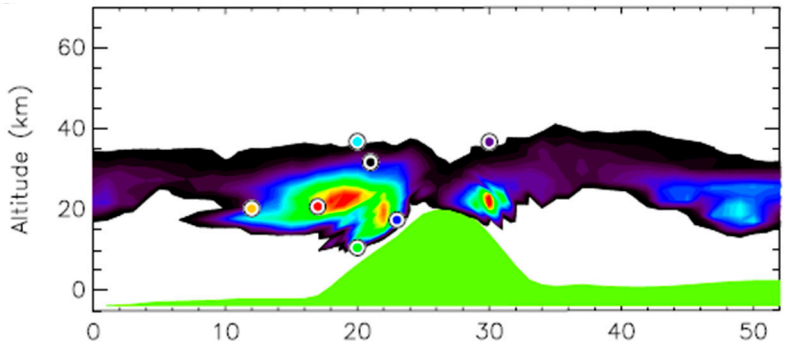



**Figure 6.** The Olympus Mons W-E cross-section of cloud mixing ratio (kg/kg) at several locations to the lee of the volcano, simulated with MRAMS (1300 local mean solar time, $L_s = 100°$). Red denotes maximum value ($5 \times 10^{-5}$) and blue minimum value ($1 \times 10^{-5}$). Reproduced from Rafkin and Michaels (2019) [37] under the Creative Commons Attribution 4.0 License.

Since the introduction of MRAMS, other mesoscale models have been developed. The LMD Martian Mesoscale Model [38] is the limited-area version, developed in 2009, of the LMD Mars GCM. It was designed with the aim of combining the improvements achieved in the mesoscale dynamical solver ARW-WRF for terrestrial applications (in terms of stability, accuracy and ergonomy), with the entire set of Martian parameterizations developed for nearly two decades in the corresponding LMD GCM, including $CO_2$ cycle, dust cycle and photochemical cycles. The usage of the same parameterization in an RCM and in the corresponding driving GCM ensures a high level of downscaling consistency. The simulations presented in [38] were performed using GCM driving data obtained at resolution 5. 625° × 3.75° for every Martian hour. Several domains were considered and centered over selected locations (e.g., Chrysie Planitia, Valles Marineris, Gusev), employing horizontal resolutions varying from 20 km to 5 km. Numerical results revealed that near-surface daily cycles of temperature, pressure, and horizontal winds are in good agreement with data from Viking and Pathfinder. Three-dimensional LES were performed over Gusev crater at a horizontal resolution of 100 m, aimed at resolving a part of a turbulence spectrum responsible for most of the energy transport within the PBL.

The MarsWRF model was also used in regional/mesoscale mode, even if not as a purely limited-area model (LAM) but instead nested into a global domain. In [24], the model was used in a very high-resolution configuration (about 490 m) centered over the Bagnold Dunes area at Gale crater. Even if starting from a global structure of the model, the study used a nested domain to explicitly represent the local processes, such as circulation around Aeolis Mons. In this way, it was possible to reproduce phenomena that are not solved at a global scale, such as diurnal cycle and turbulence in the Namib dune. The model showed a good capability in capturing the temporal structure of the circulation, even with

biases in wind speed and direction. In [39], back trajectory analyses were performed for the methane spikes detected by the MSL at Gale crater. Since high-quality wind observations on Mars were lacking, MarsWRF was used to simulate the wind fields necessary for inverse Lagrangian modeling at increasing horizontal resolutions around Gale crater. Four nested domains were employed, each increasing in spatial and temporal resolution by a factor of three relative to its parent. The innermost domain covered an area of $8.89^\circ \times 8.89^\circ$, with a horizontal resolution of $0.074^\circ$ (4.4 km) and a timestep of 2.22 s.

## 5. Open Challenges

In recent years, there has been growing research interest in exploring the Martian atmosphere. Numerical simulations have considerably supported spacecraft and telescopic observations. Despite the significant progress made, there remain numerous issues and representations of phenomena that require further improvement. A relevant part of the computational effort needed by a GCM lies in the parameterization schemes, particularly radiation, dust and cloud microphysics. Radiative transfer is one of the main forcing mechanisms and must be modeled accurately. In the Martian atmosphere, it differs from terrestrial conditions with a very low atmospheric mass, a different composition ($CO_2$-dominated) and the presence of mineral dust. Despite the significant progress achieved, the representation of radiative processes and dust is still affected by important uncertainties. In particular, the physical representation of size, shape and optical characteristics of dust is still challenging, influencing the simulated temperature structure of the atmosphere [11]. In addition, dust lifting from the surface occurs at a scale much smaller than those resolved by global models and must therefore be parameterized. A proper radiative transfer and dust representation is essential not only for climate simulations but also for short-term meteorological forecasts. Errors in dust vertical distribution can also lead to large biases in density estimates relevant to aerobraking and near-surface winds impacting rover operations. Progress in this area will likely depend on a combination of better observational constraints, improved parameterizations of small-scale processes, and the continued development of models capable of linking global circulation with mesoscale and local dynamics. Improving the representation of dust and its interaction with radiation may also benefit from emerging machine learning (ML) techniques, which can be used to develop data-driven parameterizations of sub-grid processes and to better constrain dust distributions from observations. ML represents one of the leading tools of technological advancement: in fact, while high-resolution climate models remain challenging due to the computational costs, the use of ML algorithms yields satisfactory results in terms of operational efficiency and resource consumption. For terrestrial applications, recent advances have produced ML-based models with less forecast error than single physical-based simulations [40]. On the other hand, the usage of these new techniques for Martian applications is still limited. In [41], Priyadarshini and Puri used data from the Kaggle repository (https://www.kaggle.com/imkrkannan/mars-weather-data, accessed 1 April 2026) representing the weather conditions on Mars from sol 1 (7 August 2012, on Earth) to sol 1895 (27 February 2018, on Earth) and applied different ML models (e.g., CNN, GRU, LSTM) evaluating their performances. Uprety et al. [42] employed multiple ML models for time-series forecasting to evaluate their performance against the OpenMARS dataset [43], a reanalysis that merges spacecraft observations and a Mars GCM covering over a decade of Mars years. The sensitivity of optimization solvers in the LSTM algorithm for temperature forecast over Mars was performed in [44], while a review of ML techniques for the analysis of Mars weather data is presented in [45]. These previous works give us hope that the combination of the power of artificial intelligence with the large amount of data obtained from space missions will play a crucial role in deciphering the complexities of Mars weather

patterns, but it will be essential to select relevant features and transform data appropriately to enhance the accuracy and interpretability of ML models.

The implementation of a $CO_2$ condensation scheme and its interaction with dust is another critical issue. As stated in [29], the implementation of this process will allow the simulation of specific Martian years or investigation of diurnal tides. Near-surface conditions must be effectively described to obtain an accurate prediction of surface drags, dust lifting, and tracer transport. Moreover, due to its very shallow and stratified structure, the parameterization of nocturnal boundary layer is challenging.

It is well known that grid resolutions typically employed even in mesoscale models are not sufficient for the explicit representation of the turbulent processes within the PBL. For this reason, a transition of turbulence schemes, from 1D to more complex schemes (e.g., LES), is necessary to tackle the challenges of the turbulent gray zone [35]. Encouraging results were obtained by Temel et al. [46], who performed LES computations within MarsWRF showing a good agreement between prediction of convective boundary layer height and the observational data acquired by radio occultations of Mars Express.

Data assimilation in Martian modeling is more challenging than on Earth [47], the Martian atmosphere being less chaotic and exhibiting more global features. Currently, it is still characterized by several weaknesses, since observations from instruments such as MCS, MARCI and TES are sparse in space and time, leading to large gaps, especially near the surface and in polar regions. Lander data provide in situ measurements, but only for fixed positions and not are well integrated with orbital datasets. The quality of data is also degraded by instrument biases and inter-calibration inconsistencies. Improvements could be achieved with the development of better error covariance models for Martian dynamics, including methods such as ensemble-based assimilation. The consistency could be increased with enhanced bias correction schemes and cross calibration between instruments. Observations from Emirates Mars Mission (EMM) were assimilated in 2022 into the LMD GCM using the Local Ensemble Transform Kalman Filter (LETKF) [48], demonstrating relevant improvements in the numerical representation of several phenomena, also describing how winds change during the day and night by making use of EMM's temperature observations.

## 6. Conclusions

This review provided an updated perspective of Martian climate models, highlighting their current practical applications including mission support, atmospheric reanalysis, landing site assessment, dust storm prediction, and the development of future operational forecasting capabilities for Mars. GCMs are powerful tools for understanding the Martian atmosphere. In addition to atmospheric investigations, they can be used for several purposes. For example, a recent study [49] has highlighted the importance of coupling Martian climate modeling with geological and geochemical analyses to better constrain the past environmental evolution of Mars. In particular, weathering indices derived from Gale crater sediments have been used to infer possible climate fluctuations and aqueous alteration processes in the Martian past. In a recent work, Olszewski et al. [50] used LMD and NASA M-GCM data to calibrate and validate a surface energy balance model for Mars represented by 4002 Goldberg polyhedrals.

Despite the significant progress achieved in recent decades, many issues still need to be addressed and remain active areas of research. For example, several surface features observed on Martian slopes, such as frost, gullies, slope streaks, and recurring slope lineae, are influenced by local microclimatic conditions. Until now, these processes have been investigated using one-dimensional radiative balance models. Current efforts are therefore focused on developing parameterizations capable of representing such slope-

related microclimates within three-dimensional Mars GCMs [51] to improve the realism of surface–atmosphere interactions and local-scale processes.

Many other aspects of Martian modeling need specific attention, but a detailed analysis of all of them is beyond the purpose of the present work. For example, it is worth noting that, as shown in recent video material from NASA's Mars vehicles, dust devils (particle-loaded vertical convective vortices) are very common on Mars. Since they represent a dust-lifting mechanism and possible triggers for global dust storms on Mars [52], a proper representation is needed. A first attempt was performed in [53] using the Computational Fluid Dynamics software package provided by ANSYS (ANSYS Inc., Canonsburg, PA, USA) to investigate the flow characteristics of dust devil and to lay the foundation for performing more detailed and in-depth analyses.

**Funding:** This research received no external funding.

**Data Availability Statement:** No new data were created or analyzed in this study. Data sharing is not applicable to this article.

**Acknowledgments:** During the preparation of this manuscript, the author used ChatGPT-5.3 to improve the quality of Figure 1. The author has reviewed and edited the output and takes full responsibility for the content of this publication.

**Conflicts of Interest:** The author declares no conflicts of interest. The funders had no role in the design of the study; in the collection, analyses, or interpretation of data; in the writing of the manuscript; or in the decision to publish the results.

## Abbreviations

The following abbreviations are used in this manuscript:

| | |
|---|---|
| AOPP | Atmospheric, Oceanic and Planetary Physics |
| CAP | Community Analysis Pipeline |
| CARMA | Community Aerosol Radiation Model for Atmosphere |
| CSIC | Spanish National Research Council |
| DART | Data Assimilation Research Testbed |
| EDL | Entry, Descent, Landing |
| EMM | Emirates Mars Mission |
| ESA | European Space Agency |
| GCM | General Circulation Model |
| GSFC | Goddard Space Flight Center |
| LAM | Limited-Area Model |
| LES | Large Eddy Simulation |
| LMD | Laboratoire de Meteorologie Dinamique |
| MARCI | Mars Color Imager |
| MCD | Mars Climate Database |
| MCMC | Mars Climate Modeling Center |
| MCS | Mars Climate Sounder |
| MGS | Mars Global Surveyor |
| ML | Machine Learning |
| MOLA | Mars Orbiter Laser Altimeter |
| MRO | Mars Reconnaissance Orbiter |
| MSL | Mars Science Laboratory |
| NASA | National Aeronautics and Space Administration |
| PBL | Planetary Boundary Layer |
| RCM | Regional Climate Model |
| REMS | Rover Environmental Monitoring Station |
| TES | Thermal Emission Spectrometer |

## References


1. Leovy, C. Weather and climate on Mars. *Nature* **2001**, *412*, 245–249. [CrossRef] [PubMed]
2. Leovy, C.; Mintz, Y. Numerical simulation of the atmospheric circulation and climate of Mars. *J. Atmos. Sci.* **1969**, *26*, 1166–1190. [CrossRef]
3. Pollack, J.B.; Haberle, R.M.; Schaeffer, J.; Lee, H. Simulations of the general circulation of the Martian atmosphere 1. Polar processes. *J. Geophys. Res.* **1990**, *95*, 1447–1473. [CrossRef]
4. Hourdin, F.; Phu Le Van Forget, F.; Talagrand, O. Meteorological variability and the annual surface pressure cycle on Mars. *J. Atmos. Sci.* **1993**, *50*, 3625–3640. [CrossRef]
5. Collins, M.; James, I.N. A simplified global circulation model of the Martian atmosphere. *J. Geophys. Res. Planets* **1995**, *100*, 14421–14432. [CrossRef]
6. Forget, F.; Hourdin, F.; Fournier, R.; Hourdin, C.; Talagrand, O.; Collins, M.; Lewis, S.R.; Read, P.L.; Huot, J.-P. Improved general circulation models of the Martian atmosphere from the surface to above 80 km. *J. Geophys. Res.* **1999**, *104*, 155–176. [CrossRef]
7. Lewis, S.R. Modelling the martian atmosphere. *Astron. Geophys.* **2003**, *44*, 4.6–4.14. [CrossRef]
8. Giuranna, M.; Tellmann, S.; Montmessin, F.; Belyaev, D.; Trompet, L.; Pätzold, M.; Wolkenberg, P.; Lopez-Valverde, M.A.; Korablev, O.; Forget, F. Vertical Structure of the Martian Atmosphere: The View from Mars Express. *Space Sci. Rev.* **2025**, *221*, 36. [CrossRef]
9. Lindner, B.L. The Martian polar cap: Radiative effects of ozone, clouds, and airborne dust. *J. Geophys. Res.* **1990**, *95*, 1367–1379. [CrossRef]
10. Suran, J. A calendar for Mars. *Planet. Space Sci.* **1997**, *45*, 705–708. [CrossRef]
11. Forget, F.; Millour, E.; Bierjon, A.; Delavois, A.; Fan, S.; Lange, L.; Liu, J.; Mathe, C.; Naar, J.; Pierron, T.; et al. Challenges in Mars Climate Modelling with the LMD Mars Global Climate Model, Now Called the Mars "Planetary Climate Model" (PCM). In Proceedings of the Seventh International Workshop on the Mars Atmosphere: Modelling and Observations, Paris, France, 14–17 June 2022.
12. Fouquart, Y.; Bonnel, B. Computations of solar heating of the Earth's atmosphere: A new parametrization. *Contrib. Atmos. Phys.* **1980**, *53*, 35–62.
13. Millour, E.; Forget, F.; Spiga, A.; Pierron, T.; Bierjon, A.; Montabone, L.; Lefèvre, F.; Montmessin, F.; Chaufray, J.-Y.; Lopez-Valverde, M.; et al. The Mars Climate Database (MCD version 5.2) EPSC Abstracts Vol. 10, EPSC2015-438, 2015. In Proceedings of the European Planetary Science Congress 2015, Nantes, France, 27 September–2 October 2015.
14. Mars Climate Database—Laboratoire de Météorologie Dynamique (LMD). Mars Climate Database Portal. Available online: https://www-mars.lmd.jussieu.fr/ (accessed on 16 March 2026).
15. Haberle, R. Early Mars Climate Models. *J. Geophys. Res.* **1998**, *103*, 28467–28479. [CrossRef]
16. Kahre, M.A.; Wilson, R.J.; Urata, R.A.; Brecht, A.S.; Steakley, K.E.; Batterson, C.M.; Hartwick, V.; Kling, A.; Harman, C.E.; Mester, M. The Mars Climate Modeling center at NASA AMES Research Center: Overview of recent science, model development, and progress making tools publicly available and accessible. In Proceedings of the Tenth International Conference on Mars, Pasadena, CA, USA, 22–25 July 2024.
17. Bertrand, T.; Wilson, R.J.; Kahre, M.A.; Urata, R.; Kling, A. Simulation of the 2018 global dust storm on Mars using the NASA Ames Mars GCM: A multitracer approach. *J. Geophys. Res. Planets* **2020**, *125*, e2019JE006122. [CrossRef]
18. Batterson, C.M.; Kling, A.; Hartwick, V.; Urata, R.A.; Kahre, M.A.; Wilson, R.J.; Steakley, K.; Brecht, A.S.; Harman, C.E. Increasing Access to Mars Global Climate Model (MGCM) Data with the Community Analysis Pipeline (CAP), 2023. Presented at the AGU Fall Meeting 2023, San Francisco, CA, USA, 13 December 2023. Available online: https://agu.confex.com/agu/fm23/meetingapp.cgi/Paper/1441150 (accessed on 10 March 2026).
19. Batterson, C.M.L.; Kahre, M.A.; Bridger, A.F.C.; Wilson, R.J.; Urata, R.A.; Bertrand, T. Modeling the "B" regional dust storm on Mars: Dust lofting mechanisms predicted by the new NASA Ames Mars GCM. *Icarus* **2023**, *400*, 115542. [CrossRef]
20. Hinson, D.; Wilson, R.J. Diurnal waves forced by horizontal convergence of near-surface winds on Mars. *Icarus* **2023**, *394*, 115420. [CrossRef]
21. Toigo, A.D.; Lee, C.; Newman, C.E.; Richardson, M.I. The impact of resolution on the dynamics of the martian global atmosphere: Varying resolution studies with the MarsWRF GCM. *Icarus* **2012**, *221*, 276–288. [CrossRef]
22. Richardson, M.I.; Toigo, A.D.; Newman, C.E. Planet WRF: A general purpose, local to global numerical model for planetary atmospheric and climate dynamics. *J. Geophys. Res. (Planets)* **2007**, *112*, E09001. [CrossRef]
23. Mischna, M.A.; Lee, C.; Richardson, M.I. Development of a fast, accurate radiative transfer model for the Martian atmosphere, past and present. *J. Geophys. Res.* **2012**, *117*, E10009. [CrossRef]
24. Newman, C.E.; Gómez-Elvira, J.; Marin, M.; Navarro, S.; Torres, J.; Richardson, M.I.; Battalio, J.M.; Guzewich, S.D.; Sullivan, R.; de la Torre, M.; et al. Winds measured by the Rover Environmental Monitoring Station (REMS) during the Mars Science Laboratory (MSL) rover's Bagnold Dunes Campaign and comparison with numerical modeling using MarsWRF. *Icarus* **2017**, *291*, 203–231. [CrossRef] [PubMed]

25. Wu, Z.; Richardson, M.I.; Zhang, X.; Cui, J.; Heavens, N.G.; Lee, C.; Li, T.; Lian, Y.; Newman, C.E.; Soto, A.; et al. Large eddy simulations of the dusty Martian convective boundary layer with MarsWRF. *J. Geophys. Res. (Planets)* **2021**, *126*, e2020JE006752. [CrossRef]
26. Lee, C.; Lawson, W.G.; Richardson, M.I.; Anderson, J.L.; Collins, N.; Hoar, T.; Mischna, M. Demonstration of ensemble data assimilation for Mars using DART, MarsWRF, and radiance observations from MGS TES. *J. Geophys. Res.* **2011**, *116*, E11011. [CrossRef]
27. Zhou, Y.-W.; Chow, K.-C.; Xiao, J. The Effect of Model Resolution on the Vertical and Temporal Variation in the Simulated Martian Climate. *Atmosphere* **2022**, *13*, 1736. [CrossRef]
28. Fonseca, R.M.; Zorzano, M.-P.; Martín-Torres, J. MARSWRF prediction of entry descent landing profiles: Applications to Mars exploration. *Earth Space Sci.* **2019**, *6*, 1440–1459. [CrossRef]
29. McCulloch, D.; Sergeev, D.E.; Mayne, N.; Bate, M.; Manners, J.; Boutle, I.; Drummond, B.; Kohary, K. A modern-day Mars climate in the Met Office Unified Model: Dry simulations. *Geosci. Model Dev.* **2023**, *16*, 621–657. [CrossRef]
30. McCulloch, D.; Mayne, N.; Bate, M.; Sergeev, D. Modelling an idealised Martian climate with the Unified Model: The next "giant leap" for Mars GCMs. In Proceedings of the Europlanet Science Congress 2021, Online, 13–24 September 2021. [CrossRef]
31. Hébrard, E.; Listowski, C.; Coll, P.; Marticorena, B.; Bergametti, G.; Määttänen, A.; Montmessin, F.; Forget, F. An aerodynamic roughness length map derived from extended Martian rock abundance data. *J. Geophys. Res. E Planets* **2012**, *117*, 4008. [CrossRef]
32. Lewis, S.R.; Read, P.L. An operational data assimilation scheme for the Martian atmosphere. *Adv. Space Res.* **1995**, *16*, 9–13. [CrossRef]
33. Tillman, J.E. VL1/VL2-M-MET-4-DAILY-AVG-PRESSUREV1.0, NASA [Data Set]. 1989. Available online: https://atmos.nmsu.edu/data_and_services/atmospheres_data/MARS/viking/sol_avg_sur_press_data.html (accessed on 17 March 2026).
34. Giorgi, F.; Mearns, L. Approaches to the simulation of regional climate change: A review. *Rev. Geophys.* **1991**, *29*, 191–216. [CrossRef]
35. Cinquegrana, D.; Bucchignani, E.; Montesarchio, M.; Zollo, A.L. The impact of grid resolution, turbulence schemes and soil initialization over performances of ICON model with TERRA-URB at hectometric scale. *Met. Atm. Phys.* **2026**, *138*, 3. [CrossRef]
36. Rafkin, S.C.R.; Haberle, R.M.; Michaels, T.I. The Mars Regional Atmospheric Modeling System: Model Description and Selected Simulations. *Icarus* **2001**, *151*, 228–256. [CrossRef]
37. Rafkin, S.C.R.; Michaels, T.I. The Mars Regional Atmospheric Modeling System (MRAMS): Current Status and Future Directions. *Atmosphere* **2019**, *10*, 747. [CrossRef]
38. Spiga, A.; Forget, F. A new model to simulate the Martian mesoscale and microscale atmospheric circulation: Validation and first results. *J. Geophys. Res.* **2009**, *114*, E02009. [CrossRef]
39. Luo, Y.; Mischna, M.A.; Lin, J.C.; Fasoli, B.; Cai, X.; Yung, Y.L. Mars methane sources in northwestern Gale crater inferred from back trajectory modeling. *Earth Space Sci.* **2021**, *8*, e2021EA001915. [CrossRef]
40. Price, I.; Sanchez-Gonzalez, A.; Alet, F.; Andersson, T.R.; El-Kadi, A.; Masters, D.; Ewalds, T.; Stott, J.; Mohamed, S.; Battaglia, P.; et al. Probabilistic weather forecasting with machine learning. *Nature* **2025**, *637*, 84–90. [CrossRef] [PubMed]
41. Priyadarshini, I.; Puri, V. Mars weather data analysis using machine learning techniques. *Earth Sci. Inform.* **2021**, *14*, 1885. [CrossRef]
42. Uprety, S.; Bennaceur, A.; Gavidia-Calderon, C.; Holmes, J.; Patel, M.; Rajendran, K. Weather Prediction on Mars as a Multivariate Time Series Forecasting Problem. In Proceedings of the Workshop on AI-Driven Data Engineering and Reusability for Earth and Space Sciences (DARES'25), Co-Located with the 28th European Conference on Artificial Intelligence (ECAI 2025), Bologna, Italy, 25 October 2025.
43. Holmes, J.A.; Lewis, S.R.; Patel, M.R. OpenMARS: A global record of martian weather from 1999 to 2015. *Planet. Space. Sci.* **2020**, *188*, 104962. [CrossRef]
44. Eltahan, M.; Moharm, K.; Daoud, N. Sensitivity of different optimization solvers in LSTM algorithm for temperature forecast over Mars at Jezero Crater landing site, 2020. In Proceedings of the 21st International Arab Conference on Information Technology (ACIT), Giza, Egypt, 28–30 November 2020. [CrossRef]
45. Pant, P.; Rajawat, A.S.; Goyal, S.B.; Bin Kemat, B.; Mihălţan, T.C.; Verma, C.; Răboacă, M.S. Machine Learning Techniques for Analysis of Mars Weather Data, 2023. In Proceedings of the 15th International Conference on Electronics, Computers and Artificial Intelligence (ECAI), Bucharest, Romania, 29–30 June 2023. [CrossRef]
46. Temel, O.; Senel, C.B.; Porchetta, S.; Muñoz-Esparza, D.; Mischna, M.A.; Van Hoolst, T.; van Beeck, J.; Karatekin, Ö. Large eddy simulations of the Martian convective boundary layer: Towards developing a new planetary boundary layer scheme. *Atmos. Res.* **2021**, *250*, 105381. [CrossRef]
47. Navarro, T.; Forget, F.; Millour, E.; Greybush, S.J.; Kalnay, E.; Miyoshi, T. The Challenge of Atmospheric Data Assimilation on Mars. *Earth Space Sci.* **2017**, *4*, 690–722. [CrossRef]

48. Young, R.M.B.; Millour, E.; Forget, F.; Smith, M.D.; Aljaberi, M.; Edwards, C.S.; Smith, N.; Anwar, S.; Christensen, P.R.; Wolff, M.J. First assimilation of atmospheric temperatures from the Emirates Mars InfraRed Spectrometer. *Geophys. Res. Lett.* **2022**, *49*, e2022GL099656. [CrossRef]
49. Jeon, H.; Joo, Y.J. Application of weathering indices to sedimentary records on Mars: Preliminary results. *Episodes* **2024**, *47*, 441–449. [CrossRef]
50. Olszewski, R.; Pałka, P.; Wendland, A.; Bridger, A.F.C.; Kahre, M.A.; McKay, C.P. An energy balance climate model for Mars represented by 4002 Goldberg polyhedrals with applications to ground ice re-distribution driven by obliquity cycles. *Planet. Space Sci.* **2025**, *259*, 106077. [CrossRef]
51. Lange, L.; Forget, F.; Dupont, E.; Vandemeulebrouck, R.; Spiga, A.; Millour, E.; Vincendon, M.; Bierjon, A. Modeling slope microclimates in the Mars Planetary Climate Model. *J. Geophys. Res. Planets* **2023**, *128*, e2023JE007915. [CrossRef]
52. Balme, M.; Greeley, R. Dust devils on Earth and Mars. *Rev. Geophys.* **2006**, *44*, 2005RG000188. [CrossRef]
53. Philippou, A.N.; Isaac, K.M. An Introductory Investigation of Dust Devils on Mars: Computational Fluid Dynamics Modeling, 2023, NASA-Missouri Space Grant Consortium, 34. Available online: https://scholarsmine.mst.edu/nmsgc/2023/full-schedule/34 (accessed on 8 April 2026).

**Disclaimer/Publisher's Note:** The statements, opinions and data contained in all publications are solely those of the individual author(s) and contributor(s) and not of MDPI and/or the editor(s). MDPI and/or the editor(s) disclaim responsibility for any injury to people or property resulting from any ideas, methods, instructions or products referred to in the content.